SEISMIC RETROFIT OF HOLLOW BRIDGE PIERS

Yeong-Kae Yeh
National Center for Research on Earthquake Engineering, Taipei, Taiwan
ykyeh@ncree.gov.tw

Abstract

This paper reports that circular and rectangular hollow bridge piers retrofitted by carbon fiber-reinforced plastic (CFRP) sheets were tested under a constant axial load and a cyclic reversed horizontal load to investigate their seismic behavior, including flexural ductility, dissipated energy, and shear capacity. An analytical model is also developed to predict the moment-curvature curve of sections and the lateral load-displacement relationship of piers. Based on the test results, the seismic behavior of such piers is presented. The test results are also compared to the proposed analytical model. It was found that the proposed analytical model could predict the lateral load-displacement relationship of such piers with acceptable accuracy. All in all, CFRP sheets can effectively improve both the ductility factor and shear capacity of hollow bridge piers.

INTRODUCTION

To maximize structural efficiency in terms of the strength/mass and stiffness/mass ratios and to reduce the mass contribution of the pier to seismic response (Priestly *et al*. 1996), it has been a popular engineering practice to use a hollow section for bridge piers, especially for tall piers. In contrast to the popularity in practice, researches on the structural behavior of hollow piers are limited. In the past two decades, Mander (1983) conducted an experimental investigation on four hollow column specimens; Whittaker *et al*. (1987) and Zahn *et al*. (1990) reported tests on hollow circular concrete columns; Taylor *et al*. (1994) studied the static behavior of thin-walled box piers; Matsuda *et al*. (1996) performed seismic model tests on hollow piers.

Since 1997, Mo (1998) has been proceeding with a series of both experimental and analytical investigations into the structural behavior of hollow reinforced concrete columns with an emphasis on the effect of the transverse steel configuration of hollow columns of Taiwan. The flexural response was investigated and the analytical models for prediction have been proposed (Yao 1998; Wang 1999). The shear behavior was also studied (Mo and Jeng 1999). More recently, Yeh *et al*. (2001; 2002a; b) reported tests on full-scale rectangular and circular hollow reinforced concrete bridge piers.

Recent earthquakes such as the Northridge of 1994, Kobe of 1995, and Taiwan of 1999, have repeatedly demonstrated the vulnerabilities of older reinforced concrete piers to seismic deformation demands and shear strength. Many techniques that have been implemented into the retrofit design process have been based mainly on experimental testing of scaled models of bridge structures.

Recent tests have shown that strengthening bridge piers with anyone of steel jackets (Aboutaha *et al*. 1999), fiber glass/epoxy jackets (Saadatmanesh *et al*. 1996; Xiao and Ma 1997), FRP composite jackets (Seible *et al*. 1997; Gergely *et al*. 1998), and CFRP sheets applied on hollow sections (Mo *et al*. 2004; Yeh and Mo 2004) significantly improves the flexural and shear strengths and increases the ductility of the piers.

The primary objective of this paper is to present the results of an investigation on hollow piers (Fig. 1) retrofitted with CFRP sheets. An analytical model incorporating the effect of CFRP sheets is also presented to predict the lateral loading characteristic for hollow piers. The moment-curvature relationship for the hollow section of a pier wrapped by CFRP sheets is firstly determined. Then the nonlinear lateral load-displacement relationship for hollow piers can be obtained accordingly. Also, observed experimental results from tests on two large-scale piers aimed at the confinement and shear behavior are compared to those from the proposed analytical model. The analytical model is found to be able to reflect the experimental results rather closely.

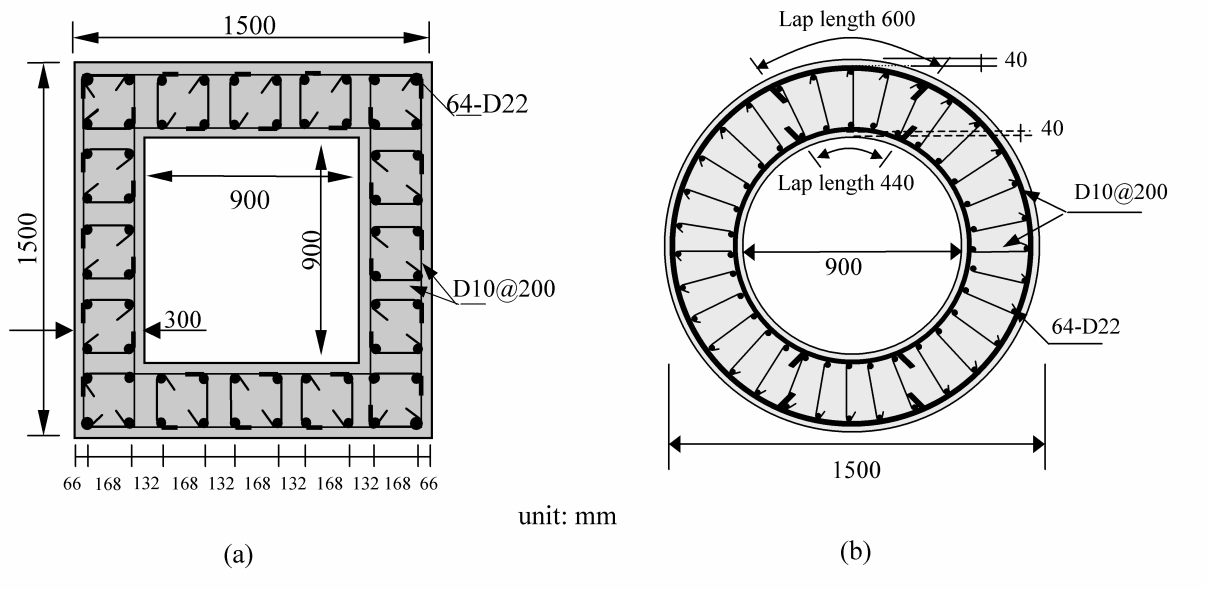

Fig. 1: Cross sections: (a) RPI and PI2; (b) RPI-C and PI2-C

ANALYTICAL MODEL

Constitutive Laws of Materials

In this investigation, the confining pressure of CFRP sheets to confined concrete is incorporated so the Mander *et al*. (1988a; b) model is employed in the analysis. The confining pressure provided by CFRP sheets and lateral steel reinforcement can increase the strength and elastic modulus of confined concrete. A typical monotonic stress-strain curve of reinforcing steel consists of three segments, namely, elastic linear branch, yield plateau, and strain hardening branch. The well-known Bauschinger effect and the low-cycle fatigue effect (Mander *et al*. 1994) are also taken into account in the analytical model.

Moment-Curvature Analysis

Based on the equilibrium of internal forces of the cross section and the assumption of the linear

distribution of normal strain (plane section remains plane after bending), the section characteristic is determined by conventional moment-curvature analysis for a cross section of RC members iteratively. Through this analysis, such sectional properties for the crack state, yield state, and ultimate state are obtained in the ascending branch, and a trilinear idealization (Mo 1994) can be made.

Load-Displacement Relationship

The displacement of piers is contributed from the flexural deformation and shear deformation. When piers are short or moderately long, the shear displacement needs to be considered. The method to determine both the flexural and shear displacements is explained below.

Flexural displacement

When the moment-curvature relationship is obtained, the load-displacement relationship can be determined by the moment area method and the curvature diagram of the column. The load-displacement relationship can be divided into the ascending and descending branches. The ascending branch can be represented by three states, namely, crack state, yield state and maximum state. Calculations for the load and corresponding displacement for each of the three states have been explained by Mo (1994). And calculations for the load and corresponding displacement for the descending branch have been explained by Yeh *et al*. (2001; 2002a; b).

Shear displacement

The shear displacement can be expressed as

$$d_v = \int_0^L e_v dl = \int_0^L P/(GA)_c \, dl \tag{1}$$

where L is the length of the pier; e_v = shear strain; P = shear force; and $(GA)_c$ is the cracked shear stiffness. It was assumed that the elastic uncracked shear stiffness is reduced in proportion to the flexural stiffness to account for the influence of cracking, which was suggested by Priestley *et al*. (1994). The load and corresponding shear displacement have been explained by Yeh and Mo (2004).

SHEAR CAPACITY

Three approaches to estimate the shear capacity are used, including ACI 318-95 Code Provisions, UCB model (Aschheim *et al*. 1992), and UCSD model (Priestley *et al*. 1993). The predicted results by the three approaches are compared with the experimental data. Except for the ACI 318-95 approach, it is recognized that the shear capacity varies with the displacement ductility factor. So the shear capacity is calculated point by point along the load-displacement curve. Considering the contribution of CFRP sheets, UCSD model (Seible *et al*. 1997) is adopted in this paper to estimate the shear capacity of reinforced concrete columns wrapped by CFRP sheets.

EXPERIMENTAL PROGRAM

Two CFRP-retrofitted reinforced concrete hollow piers (Yeh and Mo 2004) were tested under a constant axial force varying from 0.15 to 0.19 $f_c^{'} A_g$ and a cyclic reversed horizontal load. These two

specimens were compared with non-retrofitted specimens PI2-C (Yeh *et al.* 2001) and PI2 (Yeh *et al.* 2002b).

Specimens

Except the requirement of the lateral reinforcement, the column and foundation of each of the specimens were designed according to the seismic provisions (ACI 1995). Properties of the specimens are shown in Table 1. Fig. 1 indicates the dimensions of the cross section of the specimens. The diameter of the circular columns and the width of the square columns are 1500 mm; the length and wall thickness of the hollow piers are 3.5 m and 300 mm, respectively. In this paper the spacing of the confining reinforcement does not satisfy both the design requirements of ACI (1995) code, and the requirements to prevent buckling of longitudinal rebars suggested by Priestley et al. (1996), in which the spacing needs to be less than six times the diameter of longitudinal rebars. The provided shear reinforcement of the specimens with an expected shear failure is much less than that required by the ACI (1995) code. The character in the specimen designation, R or P, represents retrofit or prototype, respectively. As shown in Table 1, the second character I represents insufficient shear reinforcement when compared to the requirements of the ACI code. The last character C means the circular section. Specimen name without the last character C means the rectangular section.

Table 1: Properties of specimens

Specimen	f_c' (MPa)	P_e (kN)	$\frac{P_e}{f_c' A_g}$	L (m)	Longitudinal reinforcement			Transverse reinforcement		
					f_y (MPa)	f_u (MPa)	r_l	f_y (MPa)	Spacing (mm)	r_s
RPI*	18.0	3900	0.15	3.5	420	634	0.0169	413	200	0.00636
PI2	32.0	3600	0.078	3.5	418	626	0.0169	420	200	0.00636
RPI-C*	18.0	3900	0.19	3.5	420	634	0.0215	413	200	0.00707
PI2-C	30.9	3600	0.103	3.5	418	626	0.0215	420	200	0.00707

f_c' = concrete compressive cylinder strength; P_e = axial load; A_g = gross area of section; L = column length; f_y = steel yield strength; f_u = steel ultimate strength; r_l = ratio of longitudinal reinforcement area to gross concrete area; and r_s = ratio of volume of transverse reinforcement to the core volume confined by the transverse reinforcement.
*: specimen retrofitted by CFRP with thickness 0.55mm

Test Setup and Loading Sequence

As shown in Fig. 2, the specimen was mounted vertically on the reinforced concrete foundation, and the end of the specimen was held by two hydraulic jacks that provide a constant axial force of 3900 kN. Under the hydraulic jacks, the specimen was loaded by three actuators that were horizontally mounted to a reaction wall. Each actuator has a capacity of 1000 kN and is capable of moving the

specimen 500 mm in both push and pull directions corresponding to a column drift (ratio of horizontal displacement to column length) of 14.3%. Each specimen was instrumented with load cells, displacement transducers, and strain gauges to monitor displacements and corresponding loads as well as strains and relative deformations. A set of potentiometers were mounted on the side face of the pier parallel to the loading direction to measure vertical, horizontal, and diagonal deformations of the specimen and thus to evaluate the shear deformation (Priestley *et al*. 1994). The specimens were tested under displacement control according to a predetermined drift percentage. In each case the displacement cycle was repeated to measure the strength degradation.

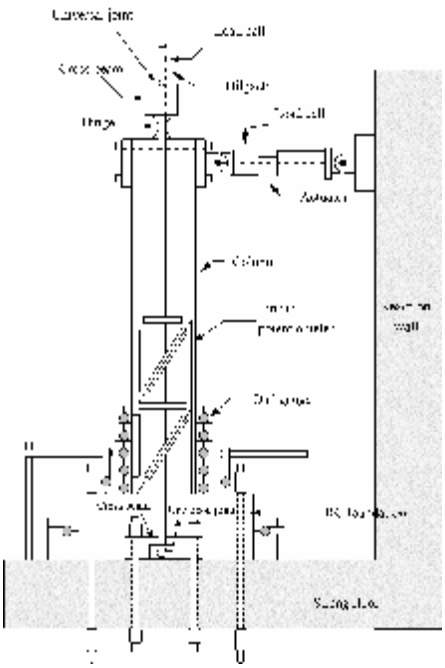

Fig. 2: Test setup

EXPERIMENTAL RESULTS

General Observations

The two retrofitted piers RPI and RPI-C developed stable responses up to certain displacement ductility levels. Plastic hinges were fully formed at the bottom end of the columns, which contributed to the development of ductile response. No shear cracks were observed on the surface of the specimens. Fig. 3 shows failure modes of specimens RPI and RPI-C. Figs. 4(a) and 5(a) show the measured hysteresis loops for lateral load versus lateral displacement relationships for rectangular and circular specimens, respectively. The dashed lines included in the load-displacement hysteresis loops of Figs. 4 and 5 indicate the ideal lateral load capacity P_i which is calculated using ACI column design method for the measured steel and concrete strengths with a strength reduction factor of unity. It can be seen from Figs. 4(a) and 5(a) that the seismic performance of the retrofitted specimen is really good when compared to the non-retrofitted specimens (Figs. 4(b) and 5(b), respectively), including ductility and dissipated energy. Although all of the specimens developed the estimated flexural strengths, their performances and ductility levels achieved were different. Table 2 gives the experimental ductility factor and dissipated energy for each of all specimens.

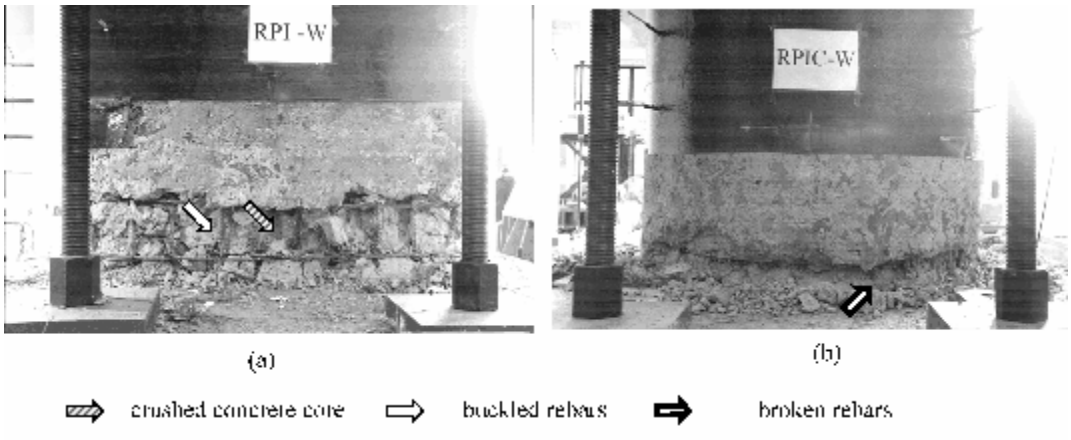

Fig. 3: Flexural failure modes: (a) crushed concrete core in RPI; (b) broken rebars in RPI-C

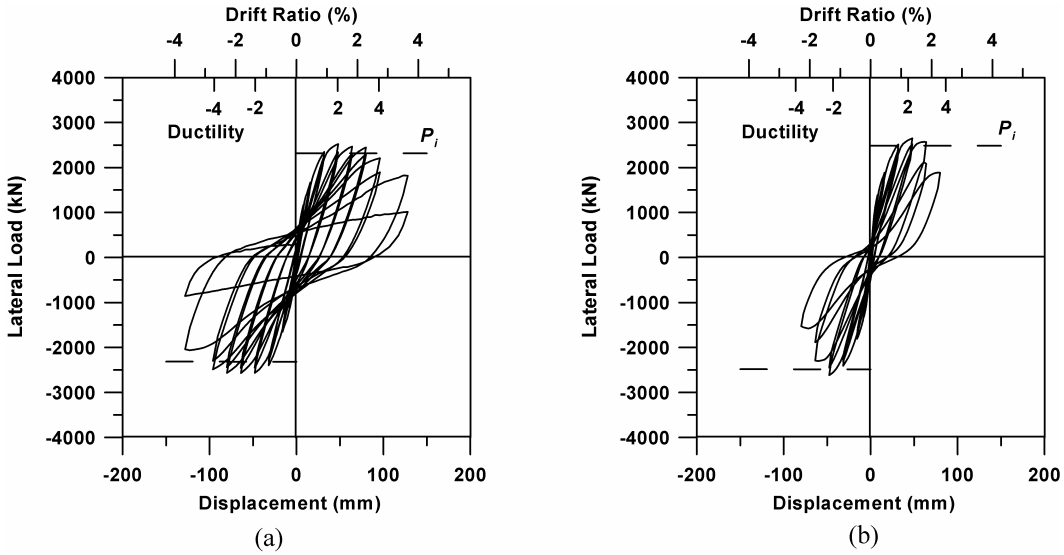

Fig. 4: Lateral load-displacement hysteresis loops of: (a) specimen RPI and (b) specimen PI2

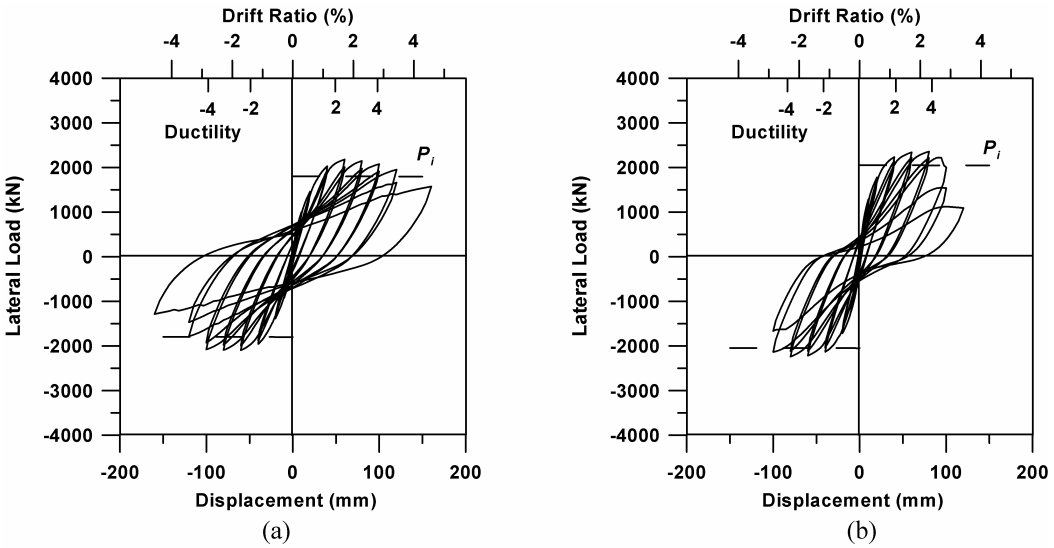

Fig. 5: Lateral load-displacement hysteresis loops of: (a) specimen RPI-C and (b) specimen PI2-C

Table 2: Experimental results

Specimen	Δ_y (mm)	P_i (kN)	Δ_u (mm)	P_m (kN)	m	Dissipated energy (kN·m)	Failure mode
RPI	23.7	2319	116.7	2544	4.9	1854	Flexure
PI2	21.6	2488	71.0	2633	3.3	541	Shear
RPI-C	24.5	1800	134.5	2138	5.5	1899	Flexure
PI2-C	20.9	2049	104.7	2299	5.0	1074	Flexure-shear

Δ_y = yield displacement; P_i = ideal lateral load capacity; P_m= maximum lateral load; and Δ_u = displacement corresponding to 0.8 P_m in the descent branch.

COMPARISON OF ANALYTICAL RESULTS WITH EXPERIMENTAL DATA

Load-Displacement Relationship

The predicted results are compared with experimental results. The total displacement is the summation of flexural deformation and shear deformation. The comparison of lateral load-displacement curves of specimen RPI is shown in Fig. 6(a). Similarly, the results of specimen RPI-C is shown in Fig. 6(b). Note that the experimental lateral load-total displacement curves in Fig. 6 are the envelopes of the lateral load-displacement hysteresis loops of each of the specimens. It is found that the predicted results are very close to the experimental results for both total displacement and flexural displacement.

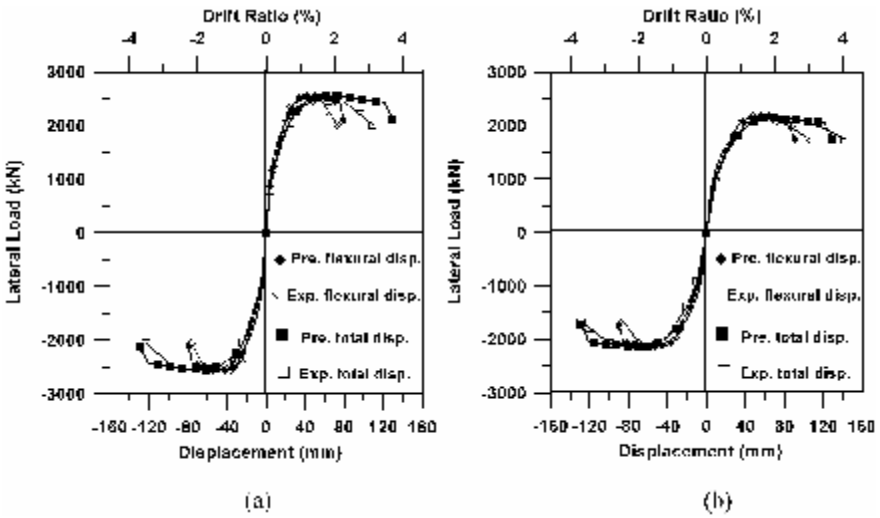

Fig. 6: Comparison of predicted and experimental lateral load-displacement curves of: (a) specimen RPI and (b) specimen RPI-C

Estimation of Shear Capacity

Figs. 7(a) and 8(a) show the experimental shear force and ductility relationships for both specimens PI2 and PI2-C, respectively. The predicted results from the ACI, UCB, and UCSD models are also shown in these figures. It can be seen from Figs. 7(a) and 8(a) that ACI 318-95 approach is too conservative. In addition, specimen PI2 failed in shear that was very close to the prediction from the UCB model (Aschheim *et al*. 1992), and specimen PI2-C failed in flexure-shear, as predicted by the UCSD model (Priestley *et al*. 1993). Both specimens RPI and RPI-C had also insufficient shear reinforcement, but were retrofitted by CFRP sheets to avoid shear failure. The comparisons between the predicted shear capacities from the Seible *et al*. model and the experimental results for these two specimens are plotted in Figs. 7(b) and 8(b). It can be seen from these figures that with the CFRP retrofits both specimens failed in flexure as predicted by the Seible *et al*. (1997) model. When specimen RPI is compared to specimen PI-2, it can be seen from the comparison of Fig. 7(b) to Fig. 7(a) that the ductility has also improved by the CFRP sheets. Since the concrete compressive strength of specimen RPI was much lower than that of specimen PI-2, the maximum shear force of specimen RPI was smaller than that of PI-2. The same conclusion can be found when specimen RPI-C is compared to PI-C. (e.g. Fig. 8(b) vs. Fig. 8(a))

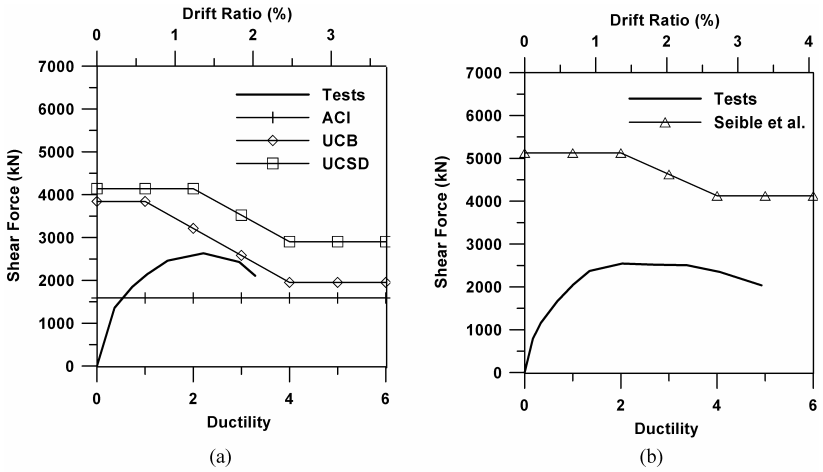

Fig. 7: Shear force-ductility relationships of: (a) specimen PI2 and (b) specimen RPI

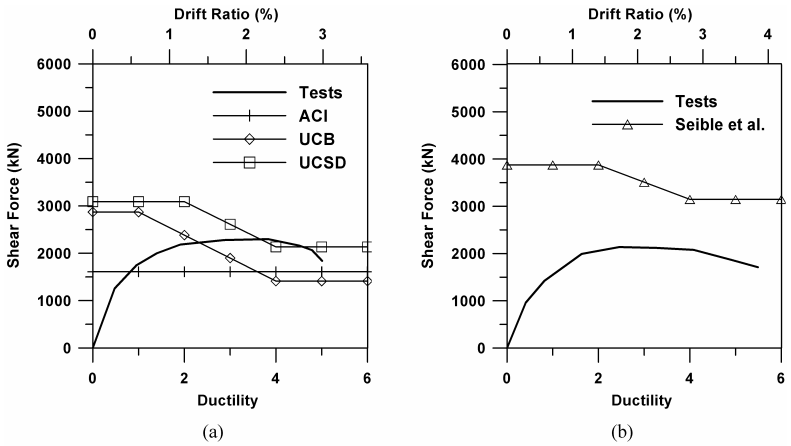

Fig. 8: Shear force-ductility relationships of: (a) specimen PI2-C and (b) specimen RPI-C

CONCLUSIONS

Based on the studies presented in this paper, the following conclusions can be made.

1. The tests verified that the UCSD model can be used for hollow sections with CFRP retrofit.
2. The tested hollow bridge piers retrofitted by CFRP sheets have acceptable seismic performance because their ductility factors range from 4.9 to 5.5.
3. CFRP sheets can effectively improve both the ductility factor and shear capacity of hollow bridge piers and successfully transform the failure mode from shear to flexure.
4. The effectiveness of confinement provided by CFRP sheets in the circular pier is better than that in the rectangular pier.
5. Both the softened branch relation and low-cycle fatigue effect need to be taken into account in the analytical model to give a good prediction.
6. The analytical model satisfactorily predicts the moment-curvature relationship and load-displacement relationship of the tested specimens with acceptable accuracy.

ACKNOWLEDGEMENTS

The research in the report was funded by National Science Council, Taiwan through grants NSC 90-2711-3-319-200-14. The authors wish to thank T.-K. Chow, C.-H. Chou, C.-C. Lin, and S. J. Wang for their assistance in construction and testing the specimens.

REFERENCES

Aboutaha, R. S., Engelhardt, M. D., Jirsa, J. O., and Kreger, M. E. (1999). "Rehabilitation of Shear Critical Concrete Columns by Use of Rectangular Steel Jackets." *ACI Struct. J.*, 96(1), 68-78.

American Concrete Institute (ACI). (1995). "Building Code Requirements for Structural Concrete (ACI 318-95) and commentary (ACI 318R-95)." Detroit.

Aschheim, M., Moehle, J. P., and Werner, S. D. (1992). "Deformability of Concrete Columns." *Project Report under Contract No. 59Q122*, California Department of Transportation, Division of Structures, Sacramento, CA.

Gergely, I., Pantelides, C. P., Nuismer, R.J., and Reaveley, L. D. (1998). "Bridge Pier Retrofit Using FRP Composites." *J. Compos. for Constr.*, ASCE, 2(4), 165-174.

Mander, J. B. (1983). "Seismic Design of Bridge Piers." Ph.D. thesis, Dept. of Civ. Engrg., University of Canterbury, Christchurch, New Zealand, Chapter 8.

Mander, J. B., Panthaki, F. D., and Kasalanati, A. (1994). "Low-Cycle Fatigue Behavior of Reinforcing Steel." *J. Mat. in Civ. Engrg.*, ASCE, 6(4), 453-468.

Mander, J. B., Priestley, M. J. N., and Park, R. (1988a). " Theoretical Stress-Strain Model for Confined Concrete." *J. Struct. Engrg.*, ASCE, 114(8), 1804-1826.

Mander, J. B., Priestley, M. J. N., and Park, R. (1988b). " Observed Stress-Strain Behavior of Confined Concrete." *J. Struct. Engrg.*, ASCE, 114(8), 1827-1849.

Matsuda, T. Yukawa, Y. Yasumatsu, T. Ishihara, S. Suda, K. Shimbo, H., and Saito, H. (1996). "Seismic Model Tests of Reinforced Concrete Hollow Piers," Proc., 12th US-Japan Bridge Engineering Workshop, 407-412.

Mo, Y. L. (1994). *Dynamic Behavior of Concrete Structures.* Elsevier Science B. V., Amsterdam,

Netherlands, 214-218.
Mo, Y. L. (1998). "Seismic Behavior of Hollow Reinforced Concrete Columns." *Research Report*, Sinotech Engineering Consultants, Taiwan (in Chinese).
Mo, Y. L., and Jeng, C. H. (1999). "Seismic Shear Behavior of Hollow Bridge Columns." *Proceedings of The First International Conference on Advances in Structural Engineering ad Mechanics*, Seoul, Korea.
Mo, Y. L., Yeh, Y.-K., and Hsieh, D. M. (2004). "Seismic Retrofit of Hollow Rectangular Bridge Columns." *J. Struct. Engrg.*, ASCE, (accepted for publication).
Priestley, M. J. N., Verma, R., and Xiao, Y. (1993). "Shear Strength of Reinforced Concrete Bridge Columns." *Second Annual Seismic Research Workshop*, Caltrans, Division of Structures, 16-18.
Priestley, M. J. N., Seible, F., and Benzoni, G. (1994). "Seismic Performance of Circular Columns with Low Longitudinal Steel Ratios," *Rep. No. SSRP-94/08*, University of California, San Diego, La Jolla, California.
Priestley, M. J. N., Seible, F., and Calvi, G. M. (1996). *Seismic Design and Retrofit of Bridges.* John Wiley & Sons, Inc..
Saadatmanesh, H., Ehsani, M. R., and Jin L. (1996). "Seismic Strengthening of Circular Bridge Pier Models with Fiber Composites." *ACI Struct. J.*, 93(6), 639-647.
Seible, F., Priestley, M. J. N., Hegemier, G. A., and Innamorato, D. (1997). "Seismic Retrofit of RC Columns with Continuous Carbon Fiber Jackets." *J. Compos. for Constr.*, ASCE, 1(2), 52-62.
Taylor, A. W., and Breen, J. E. (1994). "Design Recommendations for Thin-Walled Box Piers and Pylons." *Concrete International*, American Concrete Institute, 36-41.
Wang, S. J. (1999). "Seismic Behavior of Precast Rectangular Hollow Columns." M.S. thesis (supervised by Y.L. Mo), Dept. of Civ. Engrg., National Cheng Kung University, Taiwan (in Chinese).
Whittaker, D., Park, R., and Carr, A. J. (1987). "Experimental Tests on Hollow Circular Concrete Columns for Use in Offshore Concrete Platforms." *Proc., Pacific Conference on Earthquake Engineering*, Wairakei, , Vol. 1, 213-224.
Xiao, Y., and Ma, R. (1997). "Seismic Retrofit of RC Circular Columns Using Prefabricated Composite Jacketing." *J. Struct. Engrg.*, ASCE, 123(10), 1357-1364.
Yao, S. H. (1998). "Flexural Behavior of Rectangular Hollow Columns." M.S. thesis (supervised by Y.L. Mo), Dept. of Civ. Engrg., National Cheng Kung University, Taiwan (in Chinese).
Yeh, Y.-K., Mo, Y.L., and Yang, C.Y. (2001). "Seismic Performance of Hollow Circular Bridge Piers." *ACI Struct. J.*, 98(6), 862—871.
Yeh, Y.-K., Mo, Y.L., and Yang, C.Y. (2002a). "Seismic Performance of Rectangular Hollow Bridge Columns." *J. Struct. Engrg.*, ASCE, 128(1), 60-68.
Yeh, Y.-K., Mo, Y.L., and Yang, C.Y. (2002b). "Full-Scale Tests on Rectangular Hollow Bridge Piers." *Materials and Structures*, Vol. 35, March, 117-125.
Yeh, Y.-K., and Mo, Y. L., (2004). "Seismic Shear Retrofit of Hollow Bridge Piers." *J. Struct. Engrg.*, ASCE, (submitted).
Zahn, F. A., Park, R., and Priestley, M. J. N. (1990). "Flexural Strength and Ductility of Circular Hollow Reinforced Concrete Columns without Confinement on Inside Face." *ACI Struct. J.*, 87(2), 156-166.